Calcium Currents in Bullfrog Sympathetic Neurons

I. Activation Kinetics and Pharmacology

STEPHEN W. JONES and THEODORE N. MARKS

From the Department of Physiology and Biophysics, Case Western Reserve University, Cleveland, Ohio 44106

ABSTRACT The calcium current of bullfrog sympathetic neurons activates and deactivates rapidly ($\tau < 3$ ms). For brief depolarizations, the current can be fit reasonably well by a Hodgkin-Huxley–type model with a single gating particle of charge +3. With 2 mM Ca^{2+} as the charge carrier, half-maximal activation occurs at ~ -5 mV, near the voltage where activation and deactivation are slowest. When extracellular divalent ion concentrations are reduced, monovalent ions (e.g., Na^+ and methylammonium) produce kinetically similar inward currents. Current carried by Ba^{2+} is blocked by Cd^{2+} at micromolar concentrations, and by 100 nM ω-conotoxin. Commercially available saxitoxin blocks the current, but different batches have quantitatively different potency. The dihydropyridine agonist Bay K 8644 induces a slight shift in activation kinetics to more negative voltages, with little effect on the peak current. Nifedipine at least partially reverses the effect of Bay K 8644, but has little effect on its own. Muscarinic agonists and other ligands that inhibit the M-type potassium current of frog sympathetic neurons have weak inhibitory effects on the calcium current as well. One interpretation of these results is that the N-type calcium current predominates in these cells, with a minor contribution of L-type current.

INTRODUCTION

Calcium currents are of particular interest due to the pivotal role of intracellular calcium ions as second messengers. This and the accompanying paper (Jones and Marks, 1989) describe the kinetic and pharmacological properties of voltage-dependent calcium current in bullfrog sympathetic neurons, based on whole-cell recording from isolated cells. A preliminary communication of some of these results has appeared (Marks and Jones, 1988).

MATERIALS AND METHODS

Neurons were isolated from paravertebral sympathetic ganglia of adult bullfrogs (*Rana catesbeiana*) and maintained at 4°C as described previously (Kuffler and Sejnowski, 1983; Jones,

Address reprint requests to Dr. Stephen W. Jones, Department of Physiology and Biophysics, Case Western Reserve University, 2119 Abington Road, Cleveland, OH 44106.

J. GEN. PHYSIOL. © The Rockefeller University Press · 0022-1295/89/07/0151/17 $2.00
Volume 94 July 1989 151–167

1987*a*). Large, spherical cells (presumably B cells) were selected for recording. Currents were recorded in the whole-cell configuration, at room temperature, with an Axopatch 1B or List EPC7 patch-clamp amplifier (Hamill et al., 1981). The standard intracellular medium was 76.5 mM *N*-methyl-*D*-glucamine (NMG) chloride, 2.5 mM HEPES, 10 mM Tris-BAPTA, 5 mM Tris-ATP, and 4 mM $MgCl_2$, titrated to pH 7.2 with NMG base. The extracellular medium was 117.5 mM NMG-Cl, 2.5 mM NMG-HEPES, and 2 mM $BaCl_2$. Variations in these media are noted. Electrodes were 1.0–2.5 MΩ, producing series resistances (R_s) of 1.5–4.0 MΩ, estimated from optimal cancellation of the capacity transient. R_s compensation was nominally 80%. Data were obtained, and voltage commands were given, using pCLAMP software (CLAMPEX; Axon Instruments, Inc., Burlingame, CA) with a Labmaster A-D board. Except where noted, records were filtered at 5 kHz before sampling at 70 kHz, and digitally filtered at 3 kHz. Where noted, a brief period at the start and end of each depolarizing pulse is not shown. Records were leak subtracted using averaged (usually $n = 4$) and scaled hyperpolarizing steps of one-fourth amplitude. Voltage traces are illustrations of the protocol, not the actual recorded voltage. The holding potential was −80 mV except where noted. Cell input resistances in the linear region (hyperpolarized to −60 mV) were generally 500 MΩ–1 GΩ. Data were analyzed and plotted using pCLAMP (CLAMPAN and Clampfit), Lotus 1-2-3, and Micrografx Draw.

Drugs were applied by bath perfusion, controlled remotely by solenoid valves. Solution changes were generally complete in <1 min. Dihydropyridines were stored as 5–20 mM stocks in ethanol, and were used under dim light conditions to avoid photolysis.

Isolation of Calcium Currents

Preliminary experiments using internal Cs^+ to block potassium currents revealed calcium currents contaminated with a slowly activating outward current at positive potentials. The contaminating current, which has been noted previously (Jones, 1987*a*), was associated with slowly deactivating tail currents (several milliseconds). It has not been studied in detail, but it appears to be distinct from the eight known voltage-dependent currents of these cells. The current appears to be carried by cations, as it is also observed under conditions designed to isolate "calcium" current carried by monovalent ions, and it is not observed when internal and external cations are replaced with NMG. The contaminating current was absent with the standard recording media, but could occasionally be observed upon long depolarizations with external Ca^{2+}.

There was a very rapid outward current, lasting <1 ms, after subtraction of linear capacitance and leak, as noted for these cells (Jones, 1987*a*) and adrenal chromaffin cells (Fenwick et al., 1982). Aside from this, there was no evidence of contaminating currents with the standard recording media (see also Jones and Marks, 1989).

Accuracy of Voltage Clamp

The calcium currents in these cells can be several nanoamperes in amplitude, which raises the possibility of significant R_s error. For typical values (5 nA current, 3 MΩ R_s, 80% compensation, 80 pF cell) the estimated steady-state voltage error would be 3 mV, with a voltage-clamp time constant of 48 μs. The voltage error would be proportionately larger for the tail currents, which were quite large (occasionally saturating the patch-clamp amplifiers, which were limited to 20 nA). The observed currents are consistent with effective R_s compensation and resulting low steady-state error, as activation was smoothly graded and "notches" were not observed. Removal of R_s compensation dramatically slowed tail currents, and led to nearly all-or-none activation of the current. However, the establishment of voltage control appeared to be slightly slower than predicted, as reflected in 10–90% rise times of ~100 μs for tail

currents, even when lightly filtered (e.g., at 10 kHz, where the filter would contribute a 35-μs 10–90% rise time). This may be due to slight clamp oscillations, or to a small, slow (milliseconds) capacity transient that could not be fully compensated for.

Chemicals

Tetrodotoxin (TTX), saxitoxin (STX), BayK 8644, and nifedipine were from Calbiochem Behring Corp. (La Jolla, CA); BAPTA and EGTA acids, HEPES base, Tris-ATP, and muscarine were from Sigma Chemical Co. (St. Louis, MO); ω-conotoxin and chicken II luteinizing hormone-releasing hormone (LHRH) were from Peninsula Laboratories, Inc. (Belmont, CA); $GdCl_3$ (99.999%) from Aldrich Chemical Co. (Milwaukee, WI); $CdCl_2$ (ACS grade) from Alfa Products (Danvers, MA). Other chemicals used were Fisher Certified grade.

Computer Modeling

The AXOVACS programs (Axon Instruments, Inc.) were modified to simulate the calcium current, and to produce output files readable by Lotus 1-2-3 and pCLAMP, so that the model output could be analyzed in the same manner as experimental data. The model also incorporates the effects of series resistance on observed currents.

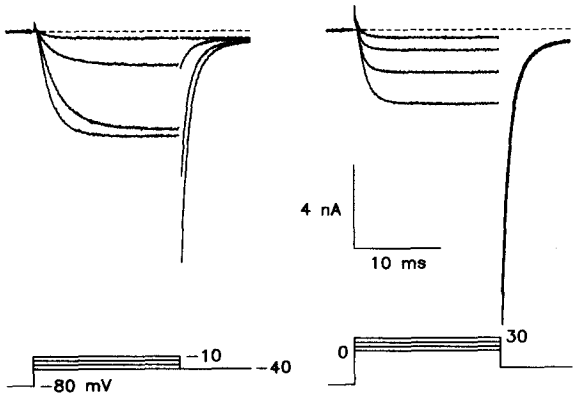

FIGURE 1. Calcium currents, with 2 mM external Ba^{2+} as the charge carrier. 250 μs were blanked at the beginning and end of each voltage step. Cell a8205; the patch pipette contained 1 mM EGTA rather than 10 mM BAPTA.

RESULTS

Activation

Fig. 1 illustrates a family of calcium currents evoked by depolarizations in 10-mV intervals from a holding potential of −80 mV, with a postpulse to −40 mV to illustrate tail currents. 2 mM Ba^{2+} was used as the charge carrier. No rapidly inactivating (T-type) current was observed. The speed of activation of the current varies with voltage, and is more rapid at extreme negative and positive potentials. The current-voltage curve (Fig. 2 *A*) has no obvious shoulders. The current is smaller with 2 mM Ca^{2+}, and the current-voltage curve is shifted to the right presumably due to surface charge effects. As expected given the nominal absence of internal permeant cations, the current shows Goldman-type rectification at positive membrane potentials, and outward currents were small even at extreme positive potentials.

Tail currents following steps to different voltages indicate the voltage dependence of activation of the calcium current (Fig. 2 B). Tail current amplitude was measured as the average of the current from 0.3 to 1.3 ms after termination of the depolarization, at a membrane potential of −40 mV, where the tail currents are relatively slow. This procedure would minimize contamination by residual uncompensated capacity transients. The relative conductance measured in this way depends on voltage in a sigmoid manner, with half-maximal activation at ~−5 mV for Ca^{2+}. The steepness of the activation curve corresponds to an e-fold change per 7–9 mV.

In some cells the activation curve measured from tail currents did not completely saturate at positive voltages, but continued to increase at least up to +80 mV. This may be due to facilitation of calcium current by large depolarizing steps (Hoshi et al., 1984; Jones and Marks, 1989).

The kinetics of the tail currents also depend on voltage (Fig. 3). Tail currents were fit reasonably well by single exponentials. Double-exponential fits to tail currents

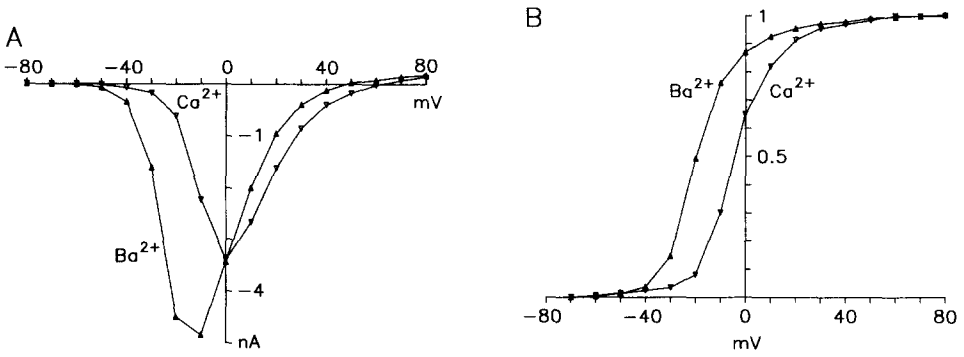

FIGURE 2. Curent-voltage relations for calcium current. Data are from the experiment illustrated in Fig. 1, and from a similar protocol recorded earlier in the same cell with 2 mM external Ca^{2+}. (*A*) Currents at the end of 15-ms steps to the voltage indicated. (*B*) Activation of calcium currents. Values are tail current amplitudes, measured at −40 mV, normalized to the value after the step to +80 mV.

revealed a small slow component (5–15% of the peak amplitude), which is not considered further here.

Time constants from single-exponential fits to tail currents are shown in Fig. 4. Also plotted are time constants for activation of currents at different voltages. Current activation was well fit by single exponentials, but the extrapolated zero time point was 300–500 μs after the initiation of the depolarization. The delay does not appear to be due to the initial rapid outward current, as it was also seen in difference currents (by subtracting the current in Cd^{2+}, STX, or ω-conotoxin from the total current; not shown).

It is noteworthy that, in the narrow voltage region where both can be accurately measured, the kinetics of activation and deactivation are similar (Fig. 4). In addition, the voltage at which the kinetics are the slowest is close to the voltage where half of the maximal conductance is observed. These results are expected from a simple Hodgkin-Huxley–style model in which the state of the channel is controlled by the

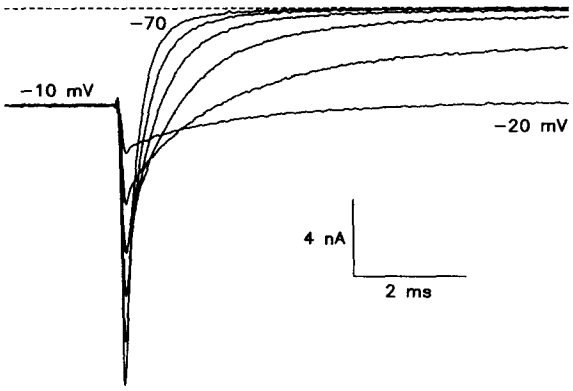

FIGURE 3. Calcium tail currents, recorded in 2 mM Ba^{2+}, from the same cell as Figs. 1 and 2. The tail currents were recorded at voltages between −20 and −70 mV, in 10-mV intervals, after 15-ms steps to −10 mV. Data were filtered at 4 kHz. The peak amplitude of the tail currents was reached at ~200 μs after the step from −10 mV in this cell.

movement of a single charged gating particle in the electrical field, according to a Boltzmann distribution. As a first approximation, gating in 2 mM Ca^{2+} can be described by:

$$a = 200\, e^{+0.06(V+5)}, \quad (1)$$

$$b = 200\, e^{-0.06(V+5)}, \quad (2)$$

where a and b are the channel opening and closing rate constants, respectively (in seconds^{-1}). The model yields $\tau = 2.5$ ms at the half-maximal activation voltage of −5 mV. The channel open probability changes e-fold for 8 mV, corresponding to an effective charge of 3 on the hypothetical gating particle. If the Goldman-Hodgkin-Katz current equation is used to approximate the voltage dependence of the conductance of open calcium channels, the shape of the current-voltage relation is well reproduced.

Monovalent Ion Currents through Calcium Channels

In experiments with internal Cs^+, the calcium current showed a clear reversal to an outward current (not shown), suggesting that Cs^+ is capable of permeating the calcium channel (Lee et al., 1985). When extracellular divalent cations were removed,

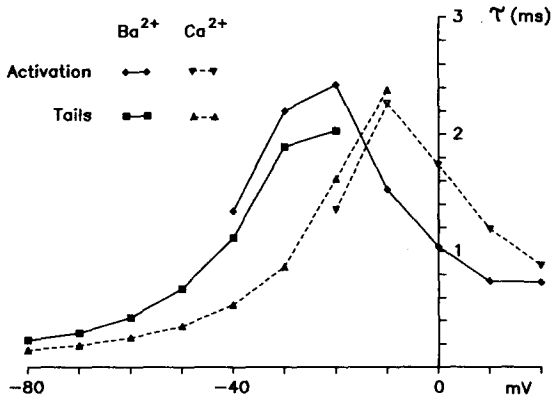

FIGURE 4. Time constants for activation and deactivation of tail currents. Time constants were from single-exponential fits to the time course of activation of calcium currents during depolarizing steps (*Activation*), or from fits to tail currents (*Tails*). Data are from the experiments of Figs. 1–3.

and 0.1 mM EGTA was added to buffer contaminating levels of divalents, little voltage-dependent current of any sort was observed with internal and external NMG. However, when NMG was replaced with Na^+, methylammonium, dimethylammonium, or Cs^+, inward currents with kinetic properties similar to those of Ba^{2+} currents could be observed (Fig. 5), as is the case for calcium currents in other cells (Hess and Tsien, 1984; McCleskey and Almers, 1985). Although the intracellular solution was nominally free of permeant ions, a clear reversal potential was observed, probably due to leakage of extracellular ions into these relatively leaky cells. These currents have been difficult to study in detail, due to the presence of a slowly activating contaminating current (see Materials and Methods), and decreased long-term survival of whole-cell recordings in zero divalent media. It was only possible to obtain these currents when the recording was initiated in zero divalent extracellular media; decreases in divalent concentrations were not tolerated well by cells under whole-cell dialysis.

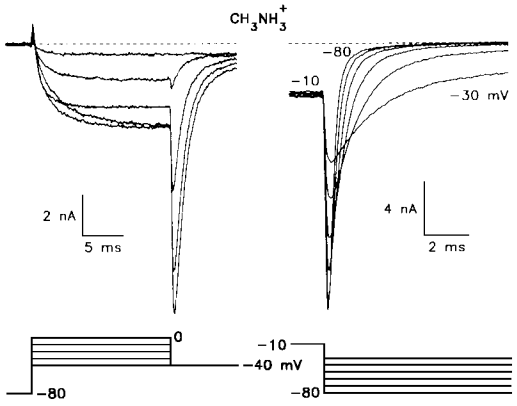

FIGURE 5. Calcium currents, with 120 mM external methylammonium as the charge carrier. The external solution also contained 0.1 mM EGTA and 2.5 mM NMG-HEPES. Records at left illustrate activation, with peak current at −20 to −10 mV, filtered at 2 kHz. Records at right illustrate tail currents after 15-ms steps to −10 mV, filtered at 4 kHz. Cell d8322.

Cd^{2+} and Other Inorganic Blockers

The calcium current is rapidly and reversibly blocked by relatively low concentrations of Cd^{2+}. The voltage and dose dependence of the effect is illustrated in Fig. 6. The dose-response curve is well fit with a Hill coefficient of 1.0 and an IC_{50} of ~400 nM. Cd^{2+} was somewhat less effective with Ca^{2+} as the charge carrier.

At submaximal doses of Cd^{2+}, the calcium current was blocked to an equivalent extent at all voltages (Fig. 7 *A*). However, the tail current amplitudes no longer varied in a sigmoid manner with voltage (Fig. 7 *B*). At the most depolarized potentials, the tail currents increased with voltage rather than remaining constant (as in the absence of Cd^{2+}). One possible explanation for this behavior is unblocking of calcium channels at extreme depolarized voltages. That interpretation is supported by a potentiation of the current in Cd^{2+} after large depolarizations (Fig. 8). Potentiation was sometimes observed under control conditions as well (Jones and Marks, 1989), but that effect was much smaller.

In the presence of Cd^{2+}, currents were slightly potentiated even after prepulses to the same potential, which was not observed under control conditions. This may

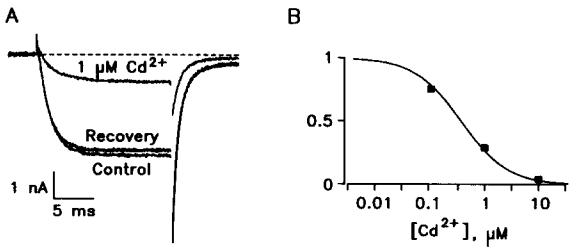

FIGURE 6. Blockade of calcium currents by Cd^{2+}. (*A*) Currents in response to steps to −10 mV, with a postpulse to −40 mV, recorded before, during, and after bath superfusion of 1 μM Cd^{2+}. 250 μs were blanked. (*B*) Dose-response relations for Cd^{2+} from the same cell. Values are the fraction of peak current remaining in Cd^{2+}, with the average of currents recorded before and after Cd^{2+} as the control value. The curve is drawn according to the law of mass action, fit by eye to an IC_{50} of 400 nM. Cell b8123; 1 mM EGTA instead of BAPTA.

reflect unblocking of the channel during the tail current, as Cd^{2+} is forced through the channel into the cell (Chow and Armstrong, 1988; Swandulla and Armstrong, 1988*a*).

Calcium currents were also blocked by millimolar concentrations of Co^{2+}, Ni^{2+} and Mn^{2+} without the voltage-dependent effects seen in Cd^{2+}. However, the trivalent cations La^{3+} and Gd^{3+} were effective at concentrations slightly lower than Cd^{2+}, and did qualitatively reproduce the phenomena (Figs. 7 and 8) seen with Cd^{2+}. The effects of the trivalent cations were only slowly reversible, but recovery could be greatly accelerated by addition of 0.1 mM EGTA to the bathing medium. Interestingly, the "unblocking" effects of extreme depolarization could be repeatedly demonstrated during washout of La^{3+} or Gd^{3+} (in the absence of EGTA).

Dihydropyridines

Bay K 8644 at micromolar concentrations caused a slight leftward shift in the current-voltage curve, which could appear as a shoulder (Fig. 9). This was associated with large, slowly activating currents around −40 mV, but less effect near the point

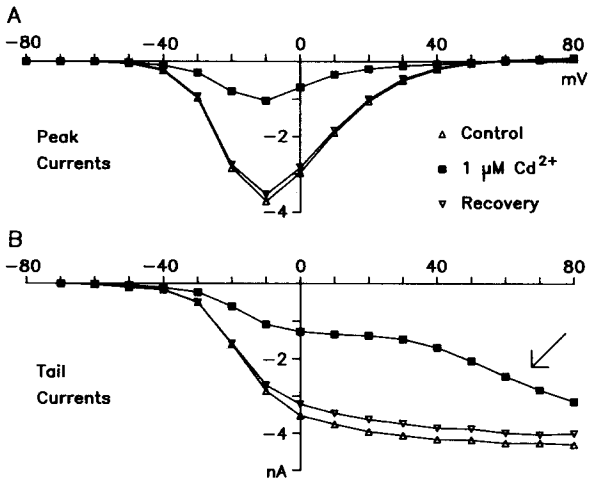

FIGURE 7. Current-voltage relations, from the response to Cd^{2+} illustrated in Fig. 6 *A*. (*A*) Values are currents at the end of 15-ms pulses to each voltage. (*B*) Tail currents, measured as the average of the current between 0.3 and 1.3 ms after the step to −40 mV from the indicated voltage. The arrow indicates an increase in the amplitude of tail currents after steps to positive potentials in Cd^{2+}.

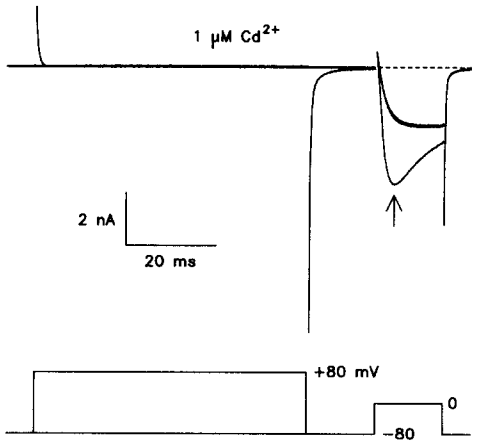

FIGURE 8. Relief of Cd^{2+} blockade by prepulses to extreme positive potentials. Three records are superimposed, one with a 60-ms prepulse to +80 mV (*arrow*). Only the postpulse to 0 mV was given during the other two records, taken 5 s before and 5 s after the record with the prepulse. Data were digitized at 20 kHz, and digitally filtered at 2 kHz, with 300 μs blanked. The full amplitude of the tail current after the step to +80 mV is not shown. The peak current was 9.5 nA before Cd^{2+} in this cell, and 9.1 nA after Cd^{2+}. Cell a8607.

of peak inward current (Fig. 10). At least one cell did show clear potentiation (~30%) at positive potentials, but that was variable. In Bay K 8644, the tail current at −40 mV has a component with kinetics slower than the normal tail current at that voltage (Fig. 10).

The effects of Bay K 8644 were slowly reversible over a period of tens of minutes. However, addition of 3–10 μM nifedipine reversed the effects of Bay K 8644. Nifedipine had little effect on its own, producing 0–25% blockade of the current (Fig. 11). Although tests of nifedipine at depolarized voltages were complicated by slow inactivation (Jones and Marks, 1989), it is clear that nifedipine was not significantly more potent from a holding potential of −40 mV than from −80 mV (Fig. 11). In cells where the effect of nifedipine was clear, the current-voltage curve was shifted slightly to the right.

STX

Some initial experiments designed to isolate calcium currents used normal internal and external concentrations of Na^+ and 1 μM STX to block voltage-dependent sodium currents. STX was used instead of TTX, due to the TTX-resistant, STX-

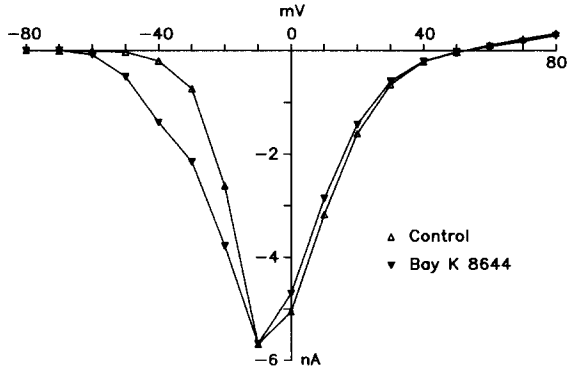

FIGURE 9. Effect of 3 μM Bay K 8644 on calcium currents. Recovery (not shown) was slow and obscured by rundown. Cell a8526.

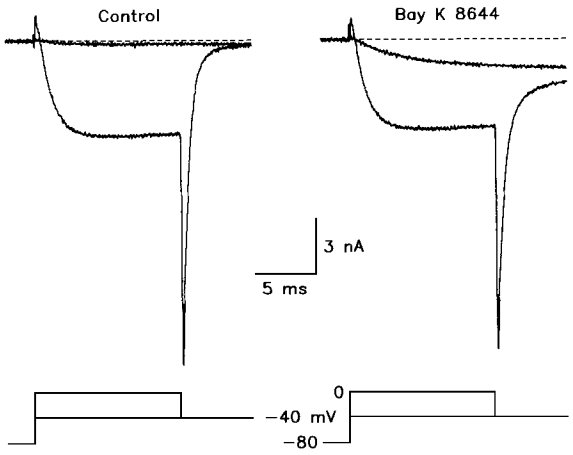

FIGURE 10. Effect on Bay K 8644 at −40 and 0 mV. Data are from the experiment of Fig 9. Data were sampled at 100 kHz with 10 kHz analog filtering, and digital filtering to 5 kHz.

sensitive sodium current of bullfrog sympathetic neurons (Jones, 1987*a*). It became clear that the amplitude of calcium currents increased when Na^+ was replaced by NMG (and STX was omitted). This turned out to be due to a blocking action of the commercial preparation of STX used (Fig. 12). The blockade was rapid in onset and recovery, showed no obvious voltage dependence (in contrast to that of Cd^{2+}, Figs. 7 and 8), and was half maximal at 400 nM STX. At 1 μM STX, 66 ± 3% (±SEM, $n = 8$) of the current was blocked with Ba^{2+}, compared with 23 ± 1% ($n = 4$) with 2 mM Ca^{2+} TTX was much less effective even at 10 μM (14 ± 6% inhibition, $n = 3$). Control experiments indicated that the other known component of the STX preparation, acetic acid, did not reduce calcium currents at the concentrations present. If enough acetic acid was added to lower the pH of the solution, the calcium current was reduced, presumably due to proton block.

However, another preparation of STX from the same source was markedly (about fourfold) less effective at blocking calcium current (Fig. 12). The two preparations blocked sodium currents with equal potency (Fig. 12). This indicates that the variation in potency against calcium currents cannot be attributed to differences in STX content.

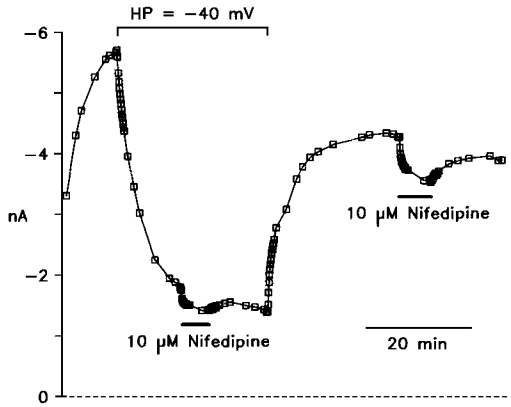

FIGURE 11. Effect of nifedipine on calcium currents. Points are the peak amplitudes during 10-ms test pulses to 0 mV. The holding potential was switched from −80 to −40 mV for the time indicated. Horizontal bars indicate the duration of bath perfusion of nifedipine. Zero time was the start of whole-cell recording. The patch pipette contained 10 mM EGTA rather than BAPTA. Cell e8927.

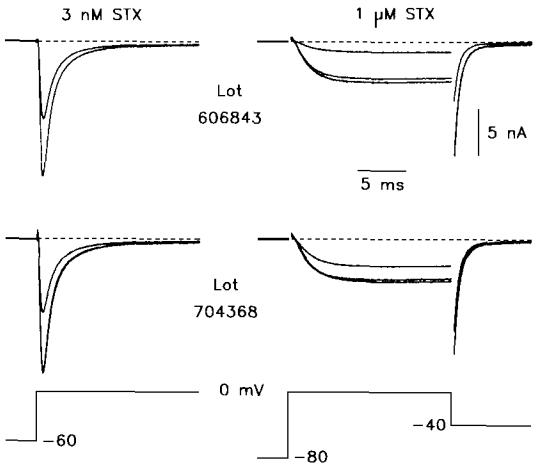

FIGURE 12. Effects of two batches of STX on sodium and calcium currents. Sodium currents were measured with 100 mM NaCl. 20 mM TEA-Cl, 2.0 mM $MnCl_2$, and 2.5 mM Na-HEPES externally. For both batches, 3 nM STX was near the IC_{50} for sodium current (*left*). However, one batch was less potent against calcium current (*right*). 300 μs were blanked from the calcium current records. All data in this figure are from cell c8318.

ω-Conotoxin

ω-Conotoxin, a peptide from the venom of a marine snail, blocked calcium currents at low concentrations, but at a very slow rate (Fig. 13). The time course of block suggests an association rate ~10^4 slower than that of Cd^{2+}. At least part of the block was slowly reversible; the true extent of reversibility is difficult to establish due to residual rundown of the calcium current (Jones and Marks, 1989). It appears that at least 90% of the calcium current is sensitive to ω-conotoxin, as was also observed for Cd^{2+} and for the STX preparation. Comparable levels of blockade were observed in the three other cells tested with ω-conotoxin.

Modulation of Calcium Current

Activation of a variety of receptors results in a slow depolarization of bullfrog sympathetic neurons. This has been attributed primarily to blockade of a specific potas-

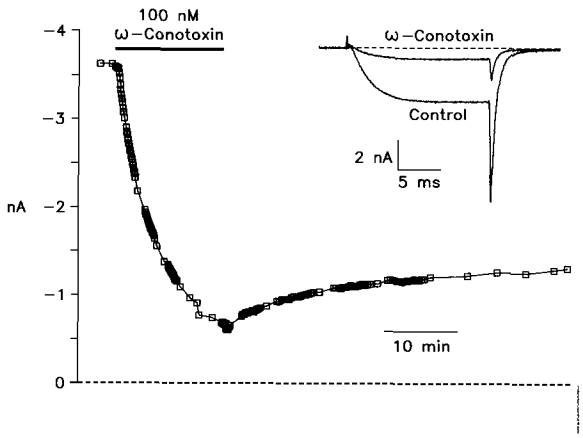

FIGURE 13. Effect of ω-conotoxin on calcium currents. The main figure shows the time course of the effect; each point is the amplitude of the current measured from a brief test pulse to the point of peak inward current (0 mV). 100 nM ω-conotoxin was applied by superfusion for the time indicated by the horizontal bar. The inset shows calcium currents recorded before ω-conotoxin and at the point of maximal effect. The voltage steps were from −80 to 0 mV with a postpulse to −40 mV. Cell d8209.

sium current, called the M-current, although other mechanisms are known to contribute (Adams et al., 1986). One possible mechanism is via modulation of calcium currents; for example, inhibition of calcium current could reduce activation of Ca^{2+}-dependent potassium currents.

It has been possible to demonstrate inhibition of calcium currents by agents that inhibit the M-current, including muscarinic agonists, extracellular ATP (Fig. 14), and LHRH. However, in contrast to the effects on M-current, the maximal effect is variable from cell to cell, and rarely reaches 50% inhibition even at maximal agonist concentrations. Fig. 14 illustrates one of the more sensitive cells encountered to date; 10–20% inhibition is a more typical result.

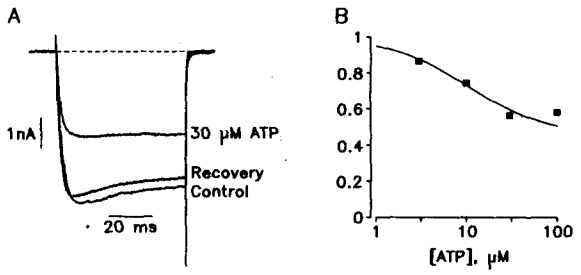

FIGURE 14. Effect of ATP on calcium currents. (*A*) Records of calcium currents, with 2 mM external Ca^{2+} and 1 mM internal EGTA, in response to 60 ms depolarizations to −10 mV, before (*Control*), during, and after (*Recovery*) bath superfusion of 30 μM ATP. The current remaining in ATP appears to show less inactivation. (*B*) Dose-response relations for ATP in the same cell. The fraction of control current is plotted against the logarithm of the ATP concentration. The effect of ATP was dose dependent but incomplete. The curve drawn corresponds to an IC_{50} of 10 μM, with 55% of the current sensitive to ATP.

DISCUSSION

At first glance, the calcium current of frog sympathetic neurons seems to result from the activity of a homogeneous population of channels, behaving in accordance with a particularly simple kinetic model. This is in agreement with the initial studies of Adams (1980), but not with more recent reports on these and other sympathetic neurons (Wanke et al., 1987; Hirning et al., 1988; Lipscombe et al., 1988). The existence of both N and L channel types at the level of unitary currents in cell-attached patches is clear (Lipscombe et al., 1988), but their quantitative contribution to the whole-cell calcium current is not established.

The apparent simplicity of the whole-cell current kinetics is consistent with the existence of a single channel type, but of course does not prove that there is only one component. Kinetic distinctions between N- and L-type current activation are small (Fox et al., 1987*b*, Lipscombe et al., 1988) and inconsistent (Wanke et al., 1987). No study to date has separated N-and L-type calcium currents in whole-cell recordings as well as might be desired, so it is still possible to maintain that there is actually only one underlying current (Swandulla and Armstrong, 1988*b*).

In the absence of kinetic differences, the issue must depend on pharmacological distinctions, which are never entirely satisfactory. The only evidence presented here for the coexistence of two current types is the effects of dihydropyridines. Bay K 8644 shifted activation of part of the current to more negative voltages (Figs. 9 and

10), and nifedipine blocked part of the control current (Fig. 11). The straightforward interpretation, which we favor, is that most of the whole-cell current is N current, and L-type calcium current is present but is only a minor component of the current in the absence of Bay K 8644. However, this is made equivocal by the complex voltage and state dependence of dihydropyridine action (Bean, 1984; Hess et al., 1984). The present data can rule out a major contribution from highly dihydropyridine-sensitive L-type channels similar to those of smooth muscle. Such currents are potentiated severalfold by Bay K 8644, and are strongly blocked by dihydropyridine antagonists at micromolar concentrations, especially from a holding potential of −40 mV (Bean et al., 1986; Caffrey et al., 1986; Marks, T. N., G. R. Dubyak, and S. W. Jones, unpublished). However, the L-type currents of neurons may be less sensitive to dihydropyridines. For example, Fox et al. (1987*a*) reported incomplete (~60%) blockade of calcium current from a holding potential of −40 mV even with 10 μM nifedipine in dorsal root ganglion neurons. So, relative insensitivity to dihydropyridines is not conclusive evidence for absence of neuronal L-type currents. Conversely, the slight sensitivity to nifedipine reported here is not conclusive evidence for the *presence* of L current. Dihydropyridines are well known to have effects on other channel types at micromolar concentrations (Nerbonne and Gurney, 1987) and block certain sodium channels even at nanomolar concentrations (Ahmed, 1988). It is not impossible that N-type channels could be blocked ~20% by 10 μM nifedipine. In favor of that interpretation, nifedipine did not have a clearly stronger blocking effect from a holding potential of −40 mV than from −80 mV (Fig. 11). That would have been expected from the voltage dependence of dihydropyridine blockade of L-type channels, and from selection for L current by steady-state inactivation of N current at −40 mV.

Even if our tentative conclusion that N current predominates in our whole-cell records is accepted, it remains possible that L current is selectively reduced under the conditions used for whole-cell recording.

Kinetics

Two aspects of the data are not predicted by the proposed kinetic model: a delay in activation of the current upon depolarization, and a small slow component of tail current deactivation. Calcium currents in several cell types have been modeled with a second-order gating process, where movement of two independent gates is necessary to open a channel (e.g., Eckert and Ewald, 1983; Kay and Wong, 1987). This would explain a delay in activation, as in the original Hodgkin and Huxley (1952) models for sodium and potassium channels. However, part of the delay observed in the present experiments can be attributed to delay in establishing voltage control. Preliminary experiments using internal cesium instead of NMG to minimize series resistance suggest that much of the delay (200–400 μs) is real, but that a simple second-order model may not be appropriate. The length of the delay did not change as strongly as predicted with voltage, even when the apparent time constant did change. Also, two-exponential fits to the time course of activation extrapolated back to positive initial values rather than to zero current. Tentatively, the calcium current is modeled here as a first-order process after a ~300-μs delay.

As noted for these cells by Adams (1980), the reasonable agreement between time

constants for activation and deactivation of currents at a given voltage is positive evidence for a first-order model (Fig. 4). It should also be noted that most of the calcium currents for which second-order models have been proposed are L-type, whereas the currents here may be predominantly N-type. Resolution of this issue will require additional study with improved voltage clamp. It is a significant question for the function of calcium channels, as a true delay in activation would affect rapid Ca^{2+}-mediated processes such as neurotransmitter release and activation of Ca^{2+}-dependent potassium channels.

The slow component of tail currents might result from the presence of an additional channel type, but similar slow components have been observed in preparations thought to have only one population of channels (Fenwick et al., 1982, Eckert and Ewald, 1983). On the other hand, under conditions reported by Nowycky et al. (1985) to activate a mixture of N and L current, tail currents in chick sensory neurons did not show evidence of multiple components (Swandulla and Armstrong, 1988*b*).

The model also predicts that tail currents become more rapid than observed at voltages hyperpolarized to −70 mV. This result might indicate that the rate constant for channel closing reaches a limiting value at negative voltages. However, this could be due to slowing of the observed tail currents by series resistance error. Computer simulations incorporating the observed cell capacitances and (compensated) R_s are consistent with the latter interpretation. Simulations do not reproduce the observed delays in activation, unless R_s is increased to levels that produce obviously bad clamp.

The model as stated is for current carried by Ca^{2+} through calcium channels. Activation of currents in 2 mM Ba^{2+} was shifted by 10–15 mV to less depolarized voltages (Figs. 2 and 4), but the currents were otherwise kinetically similar. Kinetics with monovalent ions as charge carriers were also similar except for voltage shifts. The model presented here agrees rather well with that of Adams (1980), who found slightly stronger voltage sensitivity (effective valency = 4.5), and slower kinetics (τ = 6 ms) at the half-activation point of 0 mV (with 15 mM Ca and 10 mM Mg).

Pharmacology

One of the hallmarks of N- and L-type calcium currents is high sensitivity to Cd^{2+}. The IC_{50} reported here is actually lower than reported for most other calcium currents, which can be partially explained by competition between Cd^{2+} and permeant ions, where Ca^{2+} would be expected to be more effective than Ba^{2+} (Lansman et al., 1986; Swandulla and Armstrong, 1988*a*). The blockade was fit well by the law of mass action, assuming that all of the calcium current is equally sensitive to Cd^{2+}.

Cd^{2+} appeared to reduce calcium currents equally at all voltages, with no change in kinetics, when currents were generated by depolarizing steps after holding for several seconds at −80 mV. This indicates that closed channels can be blocked; otherwise, the current would initially be large and then would show a time-dependent relaxation reflecting binding of Cd^{2+} (Chow and Armstrong, 1988). However, time-dependent relaxations could be observed after large depolarizing steps (Fig. 8). The simplest interpretation is that Cd^{2+} is driven out of the open channel at very positive potentials. The relaxation in the postpulse current in Cd^{2+} may then reflect

the kinetics of blockade of the channel by Cd^{2+}. At a Cd^{2+} concentration of 1 μM, a time constant of ~7 ms would correspond to a biomolecular rate constant of 1.4×10^8 $M^{-1}s^{-1}$ for blockade of channel by Cd^{2+} at 0 mV. However, similar effects could be observed during washout of La^{3+} and Gd^{3+}, where the free trivalent concentration should be too low to allow significant reblocking. Perhaps the blocking ion does not entirely lose its association with the channel during "unblocking" at extreme positive voltages.

The inorganic calcium channel blockers did not appear to distinguish channel subtypes in these cells, unlike the case in neuroblastoma × glioma cells, where N-type current appeared to be selectively blocked by Gd^{3+} (Docherty, 1988). This may be due to an extremely small contribution of L-type current in frog sympathetic neurons. It should be noted, however, that changes in current kinetics in Gd^{3+} could be due to voltage-dependent blockade rather than selectivity among channel types.

STX is generally thought to be entirely specific for sodium channels over potassium and calcium channels. It was thus surprising to find that commercially available STX could fully block calcium currents, albeit with approximately 100 times lower affinity than for classical sodium channels. This is particularly interesting, as frog sympathetic neurons have a TTX-resistant sodium current that is also relatively resistant to STX (IC_{50} ~100 nM; Jones, 1987*a*). This might be interpreted as additional evidence for homologies among the different sodium and calcium channels. However, the fourfold difference in potency for calcium current blockade between two batches of STX, which were equally potent for blocking sodium currents, strongly indicates that the activity of the STX preparation against calcium currents is not due to STX itself, but to some contaminant or breakdown product. At the least, this result suggests caution in the use of the high concentrations of STX necessary to fully block sodium channels. The actual active ingredient of the STX preparation might be a potent blocker of calcium currents, especially if the stated purity of the STX preparation (99%) is correct.

ω-Conotoxin, which has been reported to block both N and L channels (McCleskey et al., 1987; Hirning et al., 1988), produced a slowly and incompletely reversible blockade of at least 90% of the calcium current in frog sympathetic neurons. Kasai et al. (1987) reported variable effects of ω-conotoxin on calcium currents in chick sensory neurons, which they interpreted as irreversible blockade of N channels and incomplete and reversible blockade of L channels.

Adams et al. (1986) have argued that the primary effect of muscarinic agonists and LHRH analogues on frog sympathetic neurons is inhibition of the M-type potassium current. However, other effects have been reported (Koketsu, 1984). In mammalian sympathetic neurons, muscarinic agonists inhibit part of the calcium current, possibly by a selective action on N-type calcium current (Wanke et al., 1987). Bley and Tsien (1988) recently reported nearly complete inhibition of calcium current in frog sympathetic neurons by LHRH, but not muscarine, which was interpreted as inhibition of both L- and N-type current. The present results (Fig. 14) indicate a much weaker effect on calcium current of agents that inhibit the M-current. The reasons for this discrepancy remain to be established. Perhaps some crucial factor necessary for receptor-channel coupling is missing in the present

experiments, although M-current inhibition can be demonstrated under similar conditions (Jones, 1987*b*). On the other hand, a large inhibition of calcium current would be expected to strongly inhibit the Ca^{2+}-dependent potassium currents of these cells, whereas only weak effects are in fact observed (Adams et al., 1986). In fact, the slight inhibition of calcium currents observed here might explain the slight inhibition of the slow Ca^{2+}-dependent potassium current that is observed in response to muscarine or LHRH.

In summary, the activation kinetics and pharmacology of calcium currents in frog sympathetic neurons are consistent with the existence of a predominant class of current that resembles previously described N-type currents. This conclusion, which rests in part upon the ineffectiveness of dihydropyridine antagonists, remains tentative. Inactivation kinetics, which have also been used to distinguish types of calcium current, are discussed in the accompanying paper (Jones and Marks, 1989).

Supported by National Institutes of Health grant NS-24471.

Original version received 13 June 1988 and accepted version received 13 February 1989.

REFERENCES

Adams, P. R. 1980. The calcium current of a vertebrate neurone. *In* Physiology of Excitable Membranes. J. Salanki, editor. Akademiai Kiado, Budapest. 135–138.

Adams, P. R., S. W. Jones, P. Pennefather, D. A. Brown, C. Koch, and B. Lancaster. 1986. Slow synaptic transmission in frog sympathetic ganglia. *Journal of Experimental Biology.* 124:259–285.

Ahmed, Z. 1988. Expression of membrane currents in rat neocortical neurons in serum-free culture. I. Inward currents. *Developmental Brain Research.* 40:285–295.

Bean, B. P. 1984. Nitrendipine block of cardiac calcium channels: High-affinity binding to the inactivated state. *Proceedings of the National Academy of Sciences.* 81:6388–6392.

Bean, B. P., M. Sturek, A. Puga, and K. Hermsmeyer. 1986. Calcium channels in muscle cells isolated from rat mesenteric arteries: modulation by dihydropyridine drugs. *Circulation Research* 59:229–235.

Bley, K. R., and R. W. Tsien. 1988. LHRH and substance P inhibit N- and L-type calcium channels in frog sympathetic neurons. *Biophysical Journal.* 53:235*a*. (Abstr.)

Caffrey, J. M., I. R. Josephson, and A. M. Brown. 1986. Calcium channels of amphibian stomach and mammalian aorta smooth muscle cells. *Biophysical Journal.* 49:1237–1242.

Chow, R. H., and C. M. Armstrong. 1988. Cadmium block of calcium currents in squid neurons. *Biophysical Journal.* 53:554*a*. (Abstr.)

Docherty, R. J. 1988. Gadolinium selectively blocks a component of calcium current in rodent neuroblastoma × glioma hybrid (NG108-15) cells. *Journal of Physiology.* 398:33–47.

Eckert, R., and D. Ewald. 1983. Calcium tail currents in voltage-clamped intact nerve cell bodies of *Aplysia california*. *Journal of Physiology.* 345:533–548.

Fenwick, E. M., A. Marty, and E. Neher. 1982. Sodium and calcium channels in bovine chromaffin cells. *Journal of Physiology.* 331:599–635.

Fox, A. P., M. C. Nowycky, and R. W. Tsien. 1987*a*. Kinetic and pharmacological properties distinguishing three types of calcium currents in chick sensory neurones. *Journal of Physiology.* 394:149–172.

Fox, A. P., M. C. Nowycky, and R. W. Tsien. 1987*b*. Single channel recordings of three types of calcium channels in chick sensory neurones. *Journal of Physiology* 394:173–200.

Hamill, O. P., A. Marty, E. Neher, B. Sakmann, and F. J. Sigworth. 1981. Improved patch-clamp techniques for high-resolution current recording from cells and cell-free membrane patches. *Pflügers Archiv.* 391:85–100.

Hess, P., J. B. Lansman, and R. W. Tsien. 1984. Different modes of Ca channel gating behaviour favored by dihydropyridine Ca agonists and antagonists. *Nature.* 311:538–544.

Hess, P., and R. W. Tsien. 1984. Mechanism of ion permeation through calcium channels. *Nature.* 309:453–456.

Hirning, L. D., A. P. Fox, E. W. McCleskey, B. M. Olivera, S. A. Thayer, R. J. Miller, and R. W. Tsien. 1988. Dominant role of N-type Ca^{2+} channels in evoked release of norepinephrine from sympathetic neurons. *Science.* 239:57–61.

Hodgkin, A. L., and A. F. Huxley. 1952. A quantitative description of membrane current and its application to conduction and excitation in nerve. *Journal of Physiology.* 117:500–544.

Hoshi, T., J. Rothlein, and S. J. Smith. 1984. Facilitation of Ca^{2+} channel currents in bovine adrenal chromaffin cells. *Proceedings of the National Academy of Sciences.* 81:5871–5875.

Jones, S. W. 1987*a*. Sodium currents in dissociated bull-frog sympathetic neurones. *Journal of Physiology.* 389:605–627.

Jones, S. W. 1987*b*. Luteinizing hormone-releasing hormone as a neurotransmitter in bullfrog sympathetic ganglia. *Annals of the New York Academy of Sciences.* 519:310–322.

Jones, S. W., and T. N. Marks. 1989. Calcium currents in bullfrog sympathetic neurons. II. Inactivation. *Journal of General Physiology.* 94:00–00.

Kasai, H., T. Aosaki, and J. Fukuda. 1987. Presynaptic Ca-antagonist ω-conotoxin irreversibly blocks N-type Ca-channels in chick sensory neurons. *Neuroscience Research.* 4:228–235.

Kay, A. B., and R. K. S. Wong. 1987. Calcium current activation kinetics in isolated pyramidal neurones of the CA1 region of the mature guinea-pig hippocampus. *Journal of Physiology.* 392:603–616.

Koketsu K. 1984. Modulation of receptor sensitivity and action potentials by transmitters in vertebrate neurons. *Japanese Journal of Physiology.* 34:945–960.

Kuffler, S. W., and T. J. Sejnowski. 1983. Peptidergic and muscarinic excitation at amphibian sympathetic synapses. *Journal of Physiology.* 341:257–278.

Lansman, J. B., P. Hess, and R. W. Tsien. 1986. Blockade of current through single calcium channels by Cd^{2+}, Mg^{2+}, and Ca^{2+}. Voltage and concentration dependence of calcium entry into the pore. *Journal of General Physiology* 88:321–347.

Lee, K. S., E. Marban, and R. W. Tsien. 1985. Inactivation of calcium channels in mammalian heart cells: joint dependence on membrane potential and intracellular calcium. *Journal of Physiology.* 364:395–411.

Lipscombe, D., D. V. Madison, M. Poenie, H. Reuter, R. Y. Tsien, and R. W. Tsien. 1988. Spatial distribution of calcium channels and cytosolic calcium transients in growth cones and cell bodies of sympathetic neurons. *Proceedings of the National Academy of Sciences.* 85:2398–2402.

Marks, T. N., and S. W. Jones. 1988. Inactivation of calcium currents in bullfrog sympathetic neurons. *Biophysical Journal.* 53:562*a*. (Abstr.)

McCleskey, E. W., and W. Almers. 1985. The Ca channel in skeletal muscle is a large pore. *Proceedings of the National Academy of Sciences.* 82:7149–7153.

McCleskey, E. W., A. P. Fox, D. H. Feldman, L. J. Cruz, B. M. Olivera, R. W. Tsien, and D. Yoshikami. 1987. ω-Conotoxin: direct and persistent blockade of specific types of calcium channels in neurons but not muscle. *Proceedings of the National Academy of Sciences.* 84:4327–4331.

Nerbonne, J. M., and A. M. Gurney. 1987. Blockade of Ca^{2+} and K^+ currents in bag cell neurons of *Aplysia californica* by dihydropyridine Ca^{2+} antagonists. *Journal of Neuroscience.* 7:882–893.

Nowycky, M. C., A. P. Fox, and R. W. Tsien. 1985. Three types of neuronal calcium channel with different calcium agonist sensitivity. *Nature.* 316:440–443.

Swandulla, D., and C. M. Armstrong. 1988*a*. Kinetics of calcium channel blockade by cadmium in chick sensory neurons. *Biophysical Journal.* 53:431*a*. (Abstr.)

Swandulla, D., and C. M. Armstrong. 1988*b*. Fast-deactivating calcium channels in chick sensory neurons. *Journal of General Physiology.* 92:197–218.

Wanke, E., A. Ferroni, A. Malgaroli, A. Ambrosini, T. Pozzan, and J. Meldolesi. 1987. Activation of a muscarinic receptor selectively inhibits a rapidly inactivated Ca^{2+} current in rat sympathetic neurons. *Proceedings of the National Academy of Sciences.* 84:4313–4317.